RESULT OF THE FIRST MUON ACCELERATION WITH RADIO FREQUENCY QUADRUPOLE

R. Kitamura*, University of Tokyo, Hongo, Tokyo, Japan

M. Otani, Y. Fukao, K. Futatsukawa, N. Kawamura, T. Mibe, Y. Miyake, T. Yamazaki, KEK, Tsukuba, Ibaraki, Japan

Y. Kondo, K. Hasegawa, T. Morishita, JAEA, Tokai, Naka, Ibaraki, Japan

S. Bae, B. Kim, SNU, Seoul, Korea

G. Razuvaev, BINP SB RAS, Novosibirsk, Novosibirsk State Univ., Novosibirsk 630090 and Pulkovo Observatory, St. Petersburg, 196140, Russia.

H. Iinuma, Y. Nakazawa, Ibaraki Univ., Mito, Ibaraki, Japan

K. Ishida, RIKEN, Wako, Saitama, Japan

N. Saito, J-PARC center, Tokai, Naka, Ibaraki, Japan

Y. Sue, Nagoya Univ., Chikusa-ku, Nagoya, Japan

Abstract

Muon acceleration using radio-frequency (RF) accelerators makes it possible to precisely measure the muon anomalous magnetic moment $((g-2)_\mu)$ and the electric dipole moment (EDM). The first muon acceleration was demonstrated using an radio-frequency quadrupole (RFQ) linac. A negative muonium ion (Mu$^-$) with less than 2 keV energy was produced from an incident muon with 3 MeV energy using a thin aluminum foil target in order to cool the muon beam for the acceleration, because the designed input energy of the RFQ is 5.6 keV. The Mu$^-$ was first accelerated to 5.6 keV using an electrostatic accelerator, and was subsequently accelerated to 90 keV using the RFQ. This accelerated Mu$^-$ was selected using a diagnostic beam line and was identified based on Time-Of-Flight (TOF) measurements. The measured TOF and the beam rate of the Mu$^-$ were 828±9 ns and $(5 \pm 1) \times 10^{-4}$ Mu$^-$/sec, respectively. These two values are in close agreement with the expected values acquired from simulations results.

INTRODUCTION

More than three standard deviations between the measured value of $(g-2)_\mu$ and the predicted value from the standard model of the particle physics was reported from the E821 experiment at the Brookhaven National Laboratory (BNL) [1]. Since this discrepancy might imply the evidence of underlying physics beyond the standard model, another measurement with greater precisions, and independent of the BNL E821 is required. The aim of the J-PARC E34 experiment is to precisely measure the $(g-2)_\mu$ and the muon EDM [2]. One of the objectives is to achieve sensitivities for measurements of the $(g-2)_\mu$ and the EDM of 0.1 ppm and 10^{-21} $e \cdot$cm, respectively, in the J-PARC E34 experiment.

A unique technique which is used in the J-PARC E34 is the acceleration of muons to 212 MeV using the muon linac [3]. Muon acceleration with a RF accelerator has not been demonstrated to date. Therefore, this demonstration is

proposed as a feasibility test towards the construction of a muon linac. This paper reports on the result of the world's first muon acceleration test using a RFQ.

EXPERIMENTAL SETUP

The first muon acceleration test was performed in October 2017 at the muon beam line (muon D2 area) in the J-PARC material and life science experimental facility (MLF) [4] [5]. The total beam time was 6 days and the proton beam power during the beam time was about 300 kW. The repetition rate and the pulse mode of the proton beam were 25 Hz and single-bunch mode, respectively.

Figure 1 shows the experimental setup of the muon acceleration test. Incident positive muons with 3 MeV energy were decelerated with a SUS foil window, a Kapton degrader and a thin aluminum foil as the production target for the Mu$^-$. The thicknesses of the SUS foil, the Kapton degrader and the aluminum foil target were 50 μm, 150 μm and 200 μm, respectively. When the muon goes through the aluminum foil, the Mu$^-$, which is in the bound state of a positive muon and two electrons is produced.

The produced Mu$^-$ was extracted with an electrostatic accelerator, which is referred to as a "Soa lens" [6]. The Soa lens can accelerate and focus the Mu$^-$ beam depending on the magnitude of the voltages applied to its electrodes. Voltages of the electrodes were set in order to accelerate Mu$^-$ s to 5.6 keV, which is the designed input energy of the RFQ.

The Mu$^-$ s that are transported to the entrance of the RFQ were accelerated to 90 keV using the RFQ. After this acceleration, the Mu$^-$ s were transported to the detector using the diagnostic beam line. This beam line is composed of two magnetic quadrupoles and a magnetic bending. The diagnostic beam line selected accelerated Mu$^-$ s from penetrating positive muons, which then could become the background of the measurement. The Soa lens and the diagnostic beam line were tested using a H$^-$ beam derived from an ultra-violet light source before the acceleration tests [7].

---

* rkita@post.kek.jp

The detector was a micro channel plate (MCP) made by the Hamamatsu Co. [8] and the signal waveform from the MCP was recoded with the CAEN V1720 flash ADC [9]. The trigger of the DAQ coincided with the arrival time of the proton beam in the MLF.
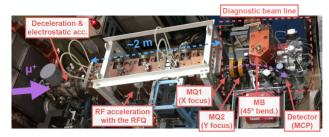

Figure 1: Experimental setup of the muon acceleration test.

Deceleration of the Muon Beam

Since the initial kinetic energy of the Mu$^-$ is less than 2 keV, it satisfies the requirement of the input energy of the RFQ. The beam rate of the Mu$^-$ produced from the thin aluminum foil target was measured at J-PARC in a preparatory experiment prior to the muon acceleration test [10]. The conditions for the incident muon beam in the muon acceleration test were the same as those for the Mu$^-$ production experiment, except for the proton beam power. The fraction of the Mu$^-$ production was estimated using the measured beam rate of the Mu$^-$ in the Mu$^-$ production experiment.

RFQ

The RFQ used for the muon acceleration test was originally designed for the J-PARC H$^-$ linac [11]. Table 1 shows the design parameters for the RFQ when the muon beam is used. The input and output β of the RFQ were determined by the vane structure, since the length of the unit cell in the vane of the RFQ is $\beta\lambda/2$, where β is the relativistic β and λ is the RF wavelength. When the muon is accelerated using this RFQ, the input and output energies are 5.6 and 90 keV, respectively.

The only variable when the RFQ is operated is the input RF power. When the muon is accelerated using this RFQ, the inter vane voltage should be scaled by the ratio of the mass of the muon to that of the H$^-$ in order to obtain the designed beam dynamics [12]. Since the input RF power is proportional to the square of the voltage, the input power is scaled by the square of the ratio of the masses. In addition, the input RF power is proportional to the length of the RFQ. This parameter was therefore scaled by the length of the RFQ. Consequently, taking the scaling of the mass between the H$^-$ and muon, and the length of the RFQ into account, the input RF power is 2.3 kW.

SIMULATION

The beam transport in the muon acceleration test was simulated using several simulation software. The incident

Table 1: Design Parameters of the RFQ Using the Muon Acceleration Test

Cavity structure	4-vane
Resonant frequency	324 MHz
Length	1973 mm
Number of cells	297
RF power	2.3 kW
Inter vane voltage	9 kV
Average bore radius	3.6 mm
Input/output β	0.01 to 0.04
Transmission*	100 %
Transverse emittance* (normalized, rms.)	0.19 π mm · mrad.
Longitudinal emittance* (normalized, rms.)	0.029 π MeV·deg.

*PARMTEQM calculation(1.0 π mm · mrad. (100 %, normalized, warterbag) injection)

muon beam was simulated using G4beamline [13]. The distribution of the initial kinetic energy of the produced Mu$^-$ s was simulated using the data for the deceleration for the low-energy proton [14]. The angular distribution was simulated using musrSim [15]. The electrostatic acceleration from the Mu$^-$ production target using the Soa lens was also simulated using musrSim, while the muon acceleration in the RFQ was simulated with PARMTEQM [16] and GPT [17]. Finally, the beam transport in the diagnostic beam line was simulated using TRACE3D [18] and PARMILA [19]. Figure 2 shows simulated phase space distributions of the accelerated Mu$^-$ at the MCP detector. The accelerated Mu$^-$ beam was transported into the effective area of the MCP as shown in Fig. 2.

RESULT

The rise time and the pulse height of the signal waveform from the MCP were reconstructed from the waveform histogram which was recorded using the flash ADC. The reconstructed rise time information was corrected by determining the *time zero*, which is the arrival time of the muon beam at the Mu$^-$ production target, in order to produce the TOF distribution. After correction of the rise time information, the threshold of the pulse height was set in order to reject the background positrons. When the threshold was 200 mV, about 80 % of the entire accelerated Mu$^-$ s remained after the threshold cut. Figure 3 shows the MCP timing distribution when the threshold was 200 mV. The peak in the distribution shows the TOF of the accelerated Mu$^-$.

The TOF and beam rate of the accelerated Mu$^-$ were estimated by the fitting. The extended-likelihood fitting was used with MINUIT [20], since the number of accelerated Mu$^-$ s was low. Assuming the bunch shape of the accelerated Mu$^-$ s is Gaussian and the same as that of the incident muon beam, and the background is the decay positron from the incident positive muon, then the fitting functions of the signal
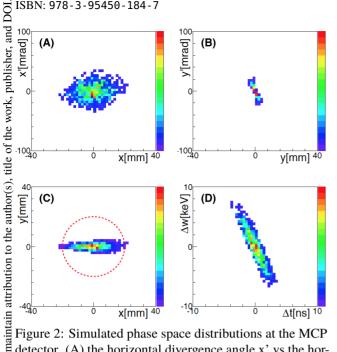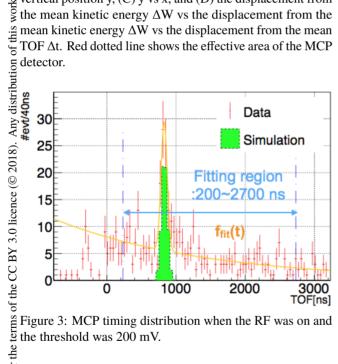
Figure 2: Simulated phase space distributions at the MCP detector. (A) the horizontal divergence angle x' vs the horizontal position x, (B) the vertical divergence angle y' vs vertical position y, (C) y vs x, and (D) the displacement from the mean kinetic energy ΔW vs the displacement from the mean kinetic energy ΔW vs the displacement from the mean TOF Δt. Red dotted line shows the effective area of the MCP detector.

Figure 3: MCP timing distribution when the RF was on and the threshold was 200 mV.

and background are defined as:

$$f_{sig}(t; \mu_{sig}, m, \sigma) = \frac{\mu_{sig}}{\sqrt{2\pi\sigma^2}} e^{\left(-\frac{(t-m)^2}{2\sigma^2}\right)} \text{ and} \quad (1)$$

$$f_{bg}(t; \mu_{bg}) = \mu_{bg} C_{bg} e^{\left(-\frac{t}{\tau}\right)}. \quad (2)$$

In the equation (1) and (2), μ_{sig} and μ_{bg} are the average of the signal and background, respectively. m and σ represent the mean and the standard deviation of the Gaussian signal function. The fitting parameters are μ_{sig}, μ_{bg}, m and σ. The τ is the mean life time of the muon and the coefficient

in the equation (2) is defined as:

$$C_{bg} \equiv \frac{1}{\tau[e^{(-\frac{t_{min}}{\tau})} - e^{(-\frac{t_{max}}{\tau})}]},$$

where t_{min} and t_{max} are the minimum and maximum of the fitting region. In Fig 3, the orange line represents the fitted function, which is the superposition of the signal and background distributions. The fitted signal peak position corresponded to the simulated signal peak position.

DISCUSSION AND CONCLUSION

The measured TOF and the beam rate of the accelerated Mu⁻ s were 828±9 ns and $(5 \pm 1) \times 10^{-4}$ Mu⁻/sec, respectively, as determined from the fitting. The expected TOF and beam rate values were 830 ns and 8×10^{-4} Mu⁻/sec from the simulation and the result of the Mu⁻ production experiment. Therefore, the measured TOF was consist with the simulated TOF and the measured beam rate agreed to the expected intensity within a factor of two.

Figure 4 shows a comparison of the MCP timing distributions for the RF-on and RF-off data, and the simulation. In the case of the RF-on data, the peak structure of the accelerated Mu⁻ was observed and the peak position of the accelerated Mu⁻ corresponded to that of the simulation. In the case of the RF-off data, no clear peak structure was observed. In conclusion, we have succeeded in accelerating muons with a RF accelerator for the first time.
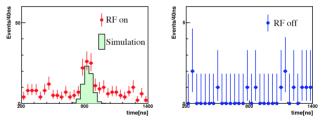

Figure 4: Comparison of MCP timing distributions between the RF-on and RF-off data, and simulation. The numbers of triggers for RF-on and RF-off data are 4×10^6 and 4×10^5, respectively.

ACKNOWLEDGEMENT

REFERENCES

[1] G.W. Bennett *et al.*, Phys. Rev. D **73**, 072003 (2006).

[2] T. Mibe *et al.* edit., J-PARC E34 Conceptual Design Report, Technical Design Report (2011).

[3] Y. Kondo *et al.*, "Re-acceleration of ultra cold muons in J-PARC muon facility", Proc. of IPAC'18, Vancouver, Canada, paper FRXGBF1, these proceedings.

[4] P. Strasser *et al.*, J. Phys.: Conf. Ser. **225** 012050 (2010).

[5] W. Higemoto *et al.*, "Materials and Life Science Experimental Facility at the Japan Proton Accelerator Research Complex IV: The Muon Facility", Quantum Beam Sci. **2017**, 1, 11.

[6] K. F. Canter, P. H. Lippel, W. S. Crane, and A. P. Mills Jr., "Positron studies of solids, surfaces and atoms"(World Scientific, Singapore, 1986) p.199.

[7] Y. Nakazawa *et al.*, "Commissioning of the diagnostic beam line for the muon RF acceleration with H- ion beam derived from the ultraviolet light", in Proc. IPAC'18, Vancouver, Canada, paper TUPAK016, these proceedings.

[8] MCP assembly F9892-21/-22 data sheet, TMCP1037E01, HAMAMATSU Photonics Co (2009).

[9] CAEN 2014 Product catalog, pp.64–67 (2014).

[10] R. Kitamura *et al.*, in Proc. of IPAC'17, Copenhagen, Denmark, pp. 2311–2313, 2017.

[11] Y. Kondo, K. Hasegawa, and A. Ueno, in Proc. of LINAC'06, Knoxville, Tennessee, pp. 749–751, 2006.

[12] Thomas P. Wangler,"*RF Linear Accelerators*", 2008, Wiley-VCH Verlag GmbH & Co.

[13] G4beamline, http://public.muonsinc.com/Projects/G4beamline.aspx

[14] M. Gonin, R. Kallenbach and P. Bochsler, Rev. Sci. Instrum. **65** 648(1994).

[15] musrSim, https://www.psi.ch/lmu/geant4-simulations

[16] K. R. Crandall *et al.*, "RFQ design codes", LA-UR-96-1836 (1996).

[17] General Particle Tracer, Pulsar Physics, http://www.pulsar.nl/gpt/

[18] K. R. Crandall and D. P. Rusthoi, "Trace 3-D Documentation", LA-UR-97-886 (1997).

[19] H. Takeda, "*Parmila*", LA-UR-98-4478 (1998).

[20] F. James, "MINUIT function minimization and error analysis–reference manual", version 94.1, CERN Program Library Long Writeup D506, https://root.cern.ch/download/minuit.pdf